THE IMPORTANCE OF HYDROGEN PARTITIONING DURING LUNAR MAGMA OCEAN CRYSTALLIZATION: IMPLICATIONS FOR CONSTRAINING THE WATER CONTENT OF THE BULK SILICATE MOON.

A. Mallik[1] (mallika@arizona.edu), S. Schwinger[2], A. Roy[1] and P. Moitra[1]. [1]Department of Geosciences, University of Arizona, [2] Institute of Planetary Research, DLR Berlin.

Introduction: Bulk H (along with D/H ratio) in the Bulk Silicate Moon (BSM) can potentially be used to: (a) derive the dynamics of the Moon-forming impact, (b) determine the origin of volatiles in the Earth-Moon system, such as volatile-rich carbonaceous chondrite versus volatile-depleted enstatite chondrite (e.g. [1], [2]). Recently measured hydrogen (H) in lunar samples have led to a range in estimates of H_2O in the BSM (5 to 1650 µg/g; [3]). These estimates rely heavily on the partition coefficients of H (D_H) between minerals and melt (where D_H = H concentration in mineral/ H concentration in the melt).

Here we demonstrate the effect of D_H between nominally anhydrous minerals (NAMs) and melt on the mantle and crustal H contents by modeling the fractional crystallization of the lunar magma ocean (LMO). We also show that along with considering D_H to best estimate the BSM H_2O content, the effect of LMO thickness and the fraction of trapped liquid should also be considered. Unless specified, H_2O content in this study refers to the equivalent content of H_2O for a given H abundance.

Methods: In our model, we use a crystallization sequence [4], where we assume a 600 km deep LMO, the lower and upper limits of D_H for each mineral-melt pair (Table 1), and vary the initial bulk H_2O (100 and 1000 ppm) assuming no residual melt in the crystal mush after compaction (Figure 1). We track the H_2O content of the crystallized phases, and compare the H_2O content of the plagioclase cumulates with the measured H_2O equivalent contents of plagioclase in FANs and Mg-suites [5, 6]. We also track the H_2O content (OH^- + molecular H_2O) of the residual liquid at each stage of crystallization, and when the dissolved H_2O content exceeds the solubility limit at a given pressure and temperature [7], we assume that the excess H_2O is degasses and outgassed efficiently from the system. We also evaluate the effect of bulk BSM or LMO H_2O content and fraction of interstitial liquid on the average crustal thickness using a combination of the codes SPICES [8] and alphaMELTS [9]. The combination of the two codes yields the best fit to experimentally produced data [10]. We have not considered the presence of molecular H_2 in the system, even though up to 20% of H in the system may be present as H_2 under LMO conditions [11]. H_2 will be considered in our future simulations.

Table 1. Range of published partition coefficients

Mineral	D_H_{min}	D_H_{max}
Olivine	0.0004 (O'Leary et al., 2010)	0.0029 (Hauri et al., 2006; Aubaud et al., 2004; Koga et al., 2003)
Cpx	0.0044 (O'Leary et al., 2010)	0.0477 (O'Leary et al., 2010)
Opx	0.003 (Dobson et al., 1995)	0.027 (Hauri et al., 2006, Aubaud et al., 2004)
Plagioclase	0.001 (Johnson & Rossman, 2003; 2004)	0.046 (Lin et al., 2019)
Ilmenite	No data (assumed zero)	No data (assumed zero)
Quartz	0.01 (Rovetta et al., 1989)	0.1 (Rovetta et al., 1989)

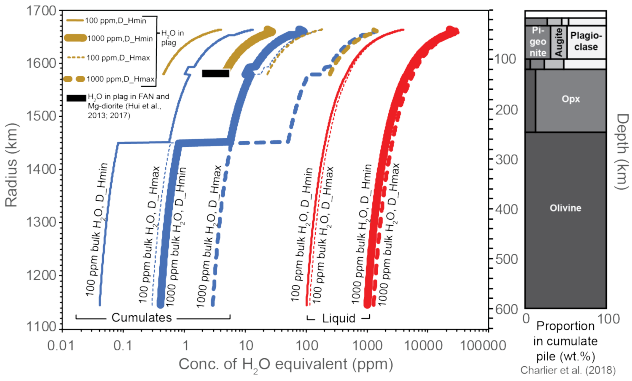

Figure 1. H_2O content in cumulates and residual liquid during crystallization of 600 km deep LMO.

Results and Discussion: H_2O content in plagioclase from FANs and Mg-suite may be explained by high bulk H_2O (1000 ppm) and lower end of D_H. If D_H is towards the upper end, then the plagioclase is explained by a low bulk H_2O content. This demonstrates the importance of constraining the D_H specific to LMO conditions in order to use H_2O in LMO products to constrain bulk H_2O in the silicate Moon. Other than tracking H_2O during LMO crystallization to constrain bulk H_2O and D_H that would best explain the H_2O content in LMO crystallization products, bulk H_2O in the system also affects the onset of plagioclase crystallization and crustal thickness [12] as fH_2O affects the ol-cpx-plagioclase cotectic [13]. To demonstrate this, we estimated the crustal thickness for two different bulk H_2O contents and two end-member D_H values, as a function of the amount of trapped interstitial liquid using the combination of SPICES and alphaMELTS. We observe that higher bulk H_2O decreases crustal thickness and the effect of D_H on crustal thickness is more pronounced for higher bulk H_2O (Figure 2a).

Crustal thickness also decreases with increasing amount of trapped interstitial liquid, as the trapped liquid results in lower availability of Ca-Al rich liquid to form a thicker crust. For a 600 km deep magma ocean, the crustal thickness given by GRAIL data [14] can be explained by lower bulk H_2O (100 ppm) and interstitial liquid less than 10%. If the initial magma ocean were deeper, a wetter Moon (500-2700 ppm H_2O) may explain the GRAIL crustal thickness (Figure 2b). Thus, in order to best estimate the bulk silicate H_2O content of the Moon, our future models will systematically investigate the role of D_H along with LMO depth and trapped liquid proportion that would best explain the H_2O contents of LMO products and GRAIL crustal thickness.

Role of molecular H_2. Under LMO crystallization conditions, molecular H_2 may consist of up to 20% of H bearing species in the system and has a lower solubility in basaltic melt (few hundred to a thousand ppm; [11]) as opposed to OH^- or molecular H_2O [7]. Thus, molecular H_2 is likely to begin degassing much earlier during LMO crystallization than H_2O. In our current simulation, H_2O degassing was reached only for higher bulk H_2O around 96% crystallization. An earlier onset of H loss from the crystallizing magma ocean due to the presence of H_2 may permit a wetter initial BSM to explain the measured H_2O equivalent contents in FANs and Mg suite rocks. Thus, we will incorporate H_2 in our future simulations to better constrain the initial H_2O in BSM.

H_2O partitioning under LMO conditions. Previous determinations of D_H between nominally anhydrous minerals (NAMs) and silicate melt (Table 1) are mostly based on terrestrial conditions and compositions, except for [15] and [16], which investigated H partitioning between plagioclase and melt applicable to lunar crust formation, i.e. at fO_2 conditions below the C-CO_2-CO (CCO) buffer and the Iron-Wustite (IW) buffer. It is observed that H in plagioclase is more compatible under reduced conditions (applicable for the Moon) than for terrestrial crust to shallow upper mantle conditions (around CCO buffer or a few log units above it). This led to the hypothesis that a redox controlled reaction in plagioclase, such as the following, may lead to increased dissolution of H in plagioclase under reduced fO_2 conditions:

$Fe^{3+} + O^{2-} + 0.5H_2O = Fe^{2+} + OH^- + 0.25O_2$ [17]

A similar enhancement of H solubility in Fe^{3+}-rich pyroxenes heated in a reduced H_2 atmosphere was observed by [18]. Also, [19] reports D_H opx/melt of 0.002 in Fe-free opx, which is an order of magnitude lower than that reported by [20], which studied pyroxene with Mg# 90-92. This likely implies that the presence of Fe in pyroxenes induces a redox controlled mechanism that renders H more compatible. It is not unreasonable to assume that a similar redox controlled mechanism would also render H more compatible in Fe-bearing olivines at low fO_2 conditions. However, oa decreased solubility of OH^- in olivine has been observed near fO_2~IW and has been attributed to changing point defects in olivine with fO_2 [21]. Thus, we aim to determine D_H during LMO conditions in an ongoing experimental study.

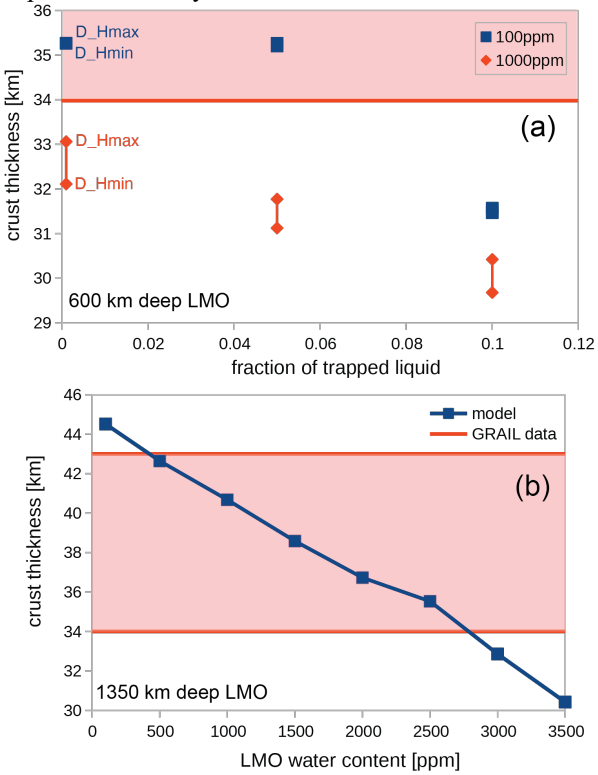

Figure 2. Crustal thickness as a function of (a) trapped liquid, bulk H_2O, D_H and (b) LMO water content.

References: [1] Barnes J. et al. (2016) *EPSL, 447*, 84–94. [2] Desch, S. J., & Robinson, K. L. (2019) *Geochemistry*, *79*(4), 125546. [3] McCubbin, F et. al. (2015) *Am. Min.*, *100*(8-9), 1668-1707. [4] Charlier, B. et al. (2018) *Geochim. Cosmochim. Acta*, *234*, 50-69. [5] Hui, H. et al. (2013) *Nat. Geosci.*, *6*(3), 177-180. [6] Hui, H et al. (2017) *EPSL*, *473*, 14-23. [7] Zhang, Y et al., (2007) *Rev. Geophys.*, *45*(4). [8] Davenport, J. D. et al. (2014) *LPSC*, 45, 1111. [9] Asimow, P. D. et al. (2004). *G-Cubed*, 5(1), Q01E16. [10] Schwinger, S., & Breuer, D. (2018) *AGUFM*, P31G-3778. [11] Hirschmann, M. M. et al., (2012) *EPSL*, 345–348, 38–48. [12] Lin, Y. et al. (2017) Nat. Geosci, 10(1), 14–18. [13] Feig, S. T. et al. (2010) *Contrib. to Mineral. Petrol.,* 160(4), 551–568. [14] Wieczorek, M. A. et al. (2013) *Science*, *339*(6120), 671-675. [15] Lin, Y. H. et al. (2019) *Geochem. Perspect. Lett.,* 10, 14–19. [16] Caseres, J. R. et al. (2017) *LPSC*, 48. [17] Mosenfelder, J. L. et al. (2020) *Geochim. Cosmochim. Acta*, 277, 87-110. [18] Skogby, H., & Rossman, G. R. (1989) *Am. Min.,* 74, 1059–1069. [19] Grant, K. J. (2004) *Geochim. Cosmochim. Acta*, 68, A34. [20] Aubaud, C. et al. (2004) *GRL*, 31(20), L20611. [21] Yang, X. (2016) *Geochim. Cosmochim. Acta*, 173, 319–336.